Imaging the drying of a colloidal suspension: Velocity field

H. Bodiguel*, J. Leng

Univ. Bordeaux/CNRS/RHODIA, LOF, UMR 5258, 178, avenue Schweitzer, F-33600 Pessac, France

A B S T R A C T

We investigate the drying kinetics of a sessile droplet containing nanoparticles. Using a fast two-color confocal imaging technique, we probe the concentration field of nanoparticles along with the velocity and mobility fields of microparticles that act as flow tracers. The flow patterns evolve according to a complex kinetics which is related to recirculating Marangoni flow coupled to the time-evolving rheology of the suspension. The drop is roughly divided in two parts: a fluid zone in which persistent recirculations flow always in the same direction, and a gelled part at the level of the corner which grows with time and also creeps under the capillary pressure.

© 2012 Elsevier B.V. All rights reserved.

1. Introduction

The drying of a sessile droplet that contains one or several solutes has been the subject of numerous studies in the past decades. It is indeed an important issue for printing [1] and coating [2] technologies to better control the resulting deposition after drying. This subject has also a large scientific and academic interest due to the inherent complexity of the problem: it couples mass and heat transfer to capillary effects, hydrodynamics and surface instabilities, rheology, etc. Although a very large body of work has been produced in the literature since the seminal work of Deegan et al. [3], only few and recent studies have focused on spatio-temporal measurements directly *inside the droplet*. Among the important issues, the existence of thermal Marangoni recirculating flow asks for some deeper work since most of the studies on this subject were devoted to the hydrodynamics of evaporating droplets of *pure liquids* [4–7] thereby ignoring the many effects of the solute on the flow.

Here, we focus on the flow patterns obtained by velocimetry measurements performed inside the drop of a colloidal suspension undergoing drying. Fluorescence indeed turns out to be a powerful tool to measure concentration fields and to image flow patterns inside the drop [7–11]. We evidence that a radial deposition flow is superimposed to persistent Marangoni recirculations which together lead to the *gelation and creeping* of the foot of the drop.

2. Materials and method

We developed an experimental technique based on fast confocal microscopy to investigate the drying of a droplet *from inside* [10]. The droplet contains a suspension of silica nanoparticles of about 6 nm radius (Ludox AM-30) that has been tagged with a fluorescent dye (rhodamine B). This operation is achieved thanks to natural adsorption of the rhodamine on the nanoparticles. The sol is then thoroughly dialyzed after adsorption in order to remove the excess of rhodamine. The tested volume fractions range from 5×10^{-3} to 0.1. We add to this suspension a small amount of fluorescent particles of 1.1 μm diameter (Fluorospheres from Invitrogen) that are tagged with fluorescein; these particles serve as tracers. The different emission spectra of the two dyes enable us to acquire the fluorescence intensity coming from the nanoparticles in one detector and simultaneously from the tracers in a second one. The size of the investigated droplet is between 2 and 3 mm, whereas the image size is 240 μm. In order to spatially map the drying, we continuously scan a plane located closed to the surface (about 10 μm above the surface) and moves the stage along a diameter of droplet. After reconstruction, we obtain an image that is 2.4 mm × 240 μm. In order to probe the kinetics of the drying, at each position 120 images are acquired at 60 Hz. A single slice therefore comprises ≈120 × 10 images which takes typically 30 s to capture (Fig. 1).

Several quantities are simultaneously measured and are described in details in reference [10]. We provide below the essential features of the measurements:

1. From the fluorescence intensity of the nanoparticles, we deduce after a calibration procedure the local nanoparticle concentration of the suspension.

* Corresponding author.
   E-mail address: hugues.bodiguel@u-bordeaux1.fr (H. Bodiguel).
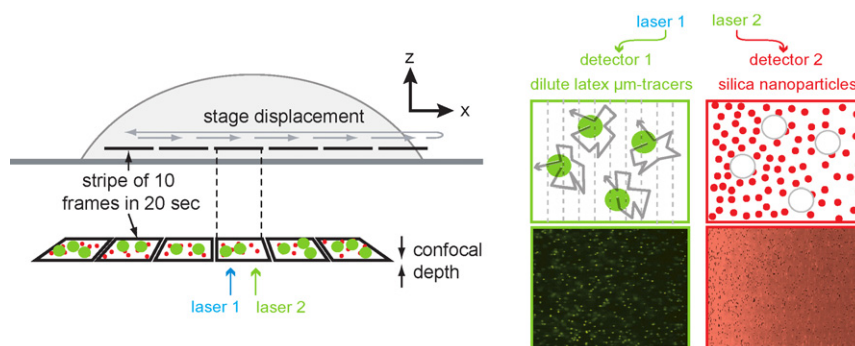
Fig. 1. Principle of the experiment: we use two-color confocal microscopy in order to scan repeatedly a slice inside a drop containing nanoparticles and tracers. We extract the concentration field of nanoparticles, the velocity field and the mobility field of tracers during the drying kinetics.

2. From the image sequences of the tracers, we use a tracking algorithm to obtain the individual displacements. We then take ensemble averages of these displacements inside rectangular boxes [of size 24 μm × 240 μm, so that we obtain a resolution of 24 μm in the radial direction]. The averaging procedure leads to local velocities measurements. Since a single plane is scanned in the experiment along the diameter of the droplet, the measurement leads to the radial component v_r of the velocity at 10 μm from the solid surface.

3. Using the same image sequences and the particles displacement but subtracting the mean displacement, we obtain the mean square diffusive displacement in the averaging boxes. This mean-square displacement is computed as a function of the correlation time τ and we verified that this mean-square displacement is proportional to the correlation time, as expected for a diffusive displacement. The self-diffusion coefficient of the tracers is then determined in each averaging box. If one then assumes that it follows Stokes–Einstein relation, the local viscosity of the suspension is given by $\mu = k_B T/6\pi D R$.

The experiments lead to the simultaneous and local measurement of the nanoparticle concentration, the viscosity and the velocity as a function of the radial position, with a spatial resolution of 25 μm. Fig. 2 shows a typical output of these experiments, namely spatio-temporal maps the three fields described above, with in each case a specific signature of the drying kinetics. We describe these features below with a special emphasis on the velocity field.

3. Results and discussion

The three fields displayed in Fig. 2 highlight specific phenomena. The intensity (Fig. 2 top) evidences the appearance and growth of a concentrated phase at the edge of the drop, which is pinned. In this growing zone, the self-diffusion coefficient of the tracers (Fig. 2 middle) vanishes within the accuracy of our detection; hereafter, we call *the gelled phase* this zone of the drop, which also corresponds to macroscopic evidences of gelation. From these measurements, we also extracted the viscosity of the suspension as a function of the particle volume fraction [10]. The suspension becomes quite viscous as the concentration is increased, reaching roughly hundred times that of water at a volume fraction of ≈8%, probably due to high electrostatic repulsions held by the small nanoparticles. We also identified recirculations inside the drop probably due to thermal effects.

The velocity diagram (Fig. 2 bottom) shows that the flow in vicinity of the solid surface is directed from the center to the edge of the drop. We focus in the following on the description of the velocity

fields as a function of space and time, and we characterized them for several initial concentrations of nanoparticles (NPs).

3.1. Mean velocity

We first describe the mean radial velocity (averaged over r) as a function of time for several initial concentrations, as shown in Fig. 3 (top). Note first that we take the origin of time at the end of the drying (i.e., we plot $\bar{v}$ against $t - t_f$) where we measured the final drying time t_f. The latter is a function of the initial NPs concentration and we observe that this shift not only permits to collapse all the data but also evidences *three different regimes*, regardless of the initial concentration. At short times, the mean velocity remains at its initial value (≈5 μm/s); Then, roughly 500 s before the end of the drying, it starts decreasing; Eventually, in the last 150 s, it is roughly constant and quite small. The same observation is obtained if one looks at the position of the edge of the gelled phase as a function of time (again from the end of drying) which is also reported in Fig. 3
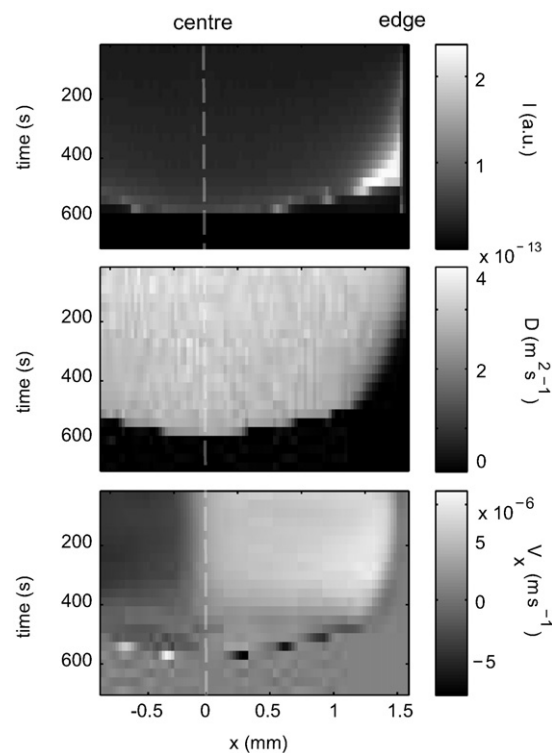
Fig. 2. Typical outcome of the experiment. From top to bottom, spatio-temporal diagrams of: the fluorescence intensity, the self-diffusion coefficient of the tracers, and the velocity along the *x*-axis.
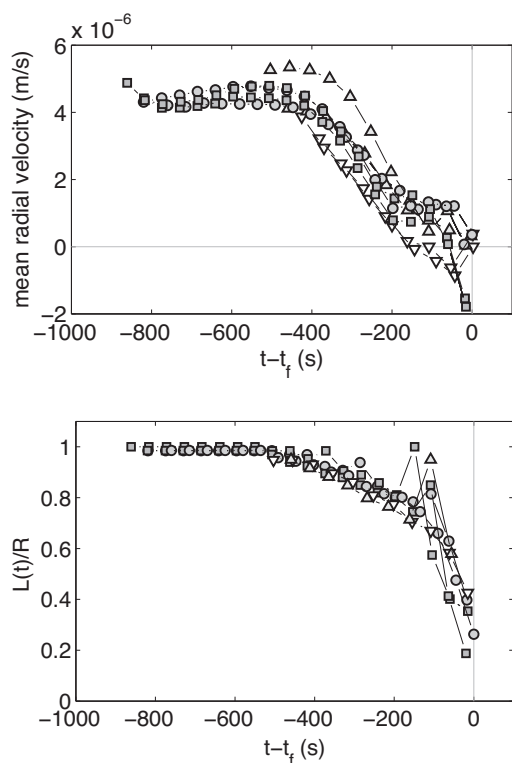
Fig. 3. Top – Mean value of the radial component of the velocity as a function of time, for 8 different droplets having the following initial volume fractions: 0.25% (squares), 1.25% (circles), 2.5% (up triangles) and 5% (down triangles). Bottom – Reduced radial position of the edge of the gelled phase as a function of the drying time.

(bottom). We define it via a thresholding of D, the self-diffusion coefficient, which is assumed to represent a gelled phase when it falls below 0.5×10^{-13} m^2/s [10]. We recover a good collapse of the deposition kinetics $L(t)$ when seen from the end of the drying, with also a deposition kinetics which starts with the second regime of the velocity field.

Importantly, both the mean features of the flow and of the deposition are, in a first approximation, independent on the initial concentration of NPs.

3.2. Local velocity

At 10 μm from the solid surface, the order of magnitude of the velocity is rather high (a few micrometers per second). Since the droplet height is of the order of a few hundreds of micrometer at the beginning of the experiment, we expect that the mean velocity along the thickness to be about 10 times higher than the velocity measured just above the solid surface. If the flow inside the droplet was due to the evaporation flux only, we would have expected a mean velocity on the order of $v \sim R/t_e$ with R the radius of the drop and t_e the typical evaporation time. The mean velocity along the thickness would have then been on the order of 1 μm/s, i.e., much lower than the experimental data. It might thus be concluded that there exists an additional flow, likely to be due to a Marangoni stress, as pointed out by several authors [4–6]. Furthermore, the velocity fields displayed in Figs. 4 and 5 indicate that there is a recirculating flow going from the center to the edge near the surface. Indeed, the z-component of the velocity is negative at the center and positive near the droplet edge. Comparison of the velocity fields to the analytic expression provided by Huh and Larson [4] (not shown, see reference [10]) leads to an estimate of the Marangoni number
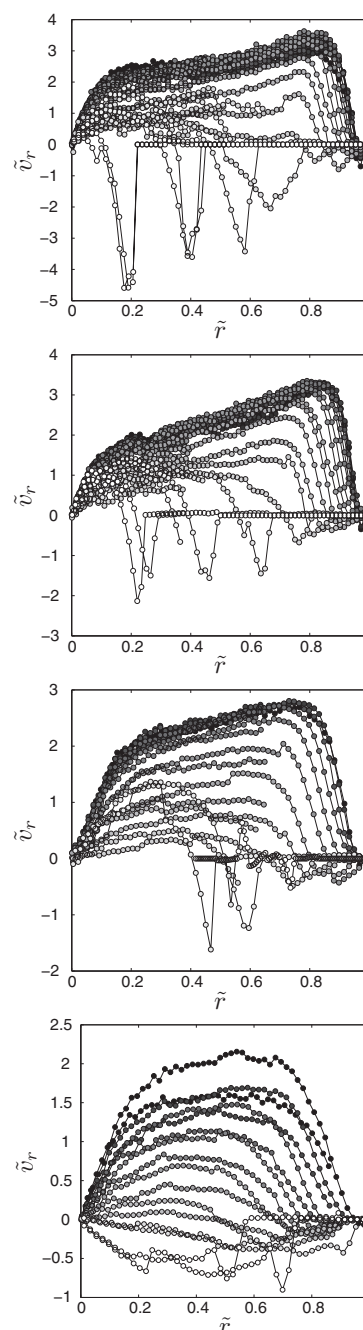

Fig. 4. Radial velocity $\tilde{v}_r$ as a function of the distance $\tilde{r}$ from the center, and at $z = 10$ μm. From the top to the bottom, the initial volume fractions of NPs are 0.25%, 1.25%, 2.5% and 5% respectively. The grayscale of the symbols indicate the time of the velocity data, the darkest the soonest (the white symbols are very close to the total drying time, while the black one are taken at the beginning of drying). The distance is normalized by the drop radius R, and the velocity by R/t_f, where t_f is the total drying time; The order of magnitude of R/t_f is between 1 and 3 μm/s.

of order of 10^3 based on temperature effect on surface tension of order of 0.2 mN/m/K and temperature gradients of order of 10 K/m.

As time passes during he course of drying, it is interesting to note that the Marangoni recirculating flow remains unchanged even though its amplitude decreases. This slowing down might be explained at first by the decrease of the Marangoni number since the viscosity of the solution is constantly increasing and the thickness is decreasing in time. According to the mean velocity variations shown in Fig. 3, the slowing down starts when the volume fraction is above 5%. Since correlatively the viscosity increases very rapidly

4   *H. Bodiguel, J. Leng / Chemical Engineering and Processing xxx (2012) xxx–xxx*
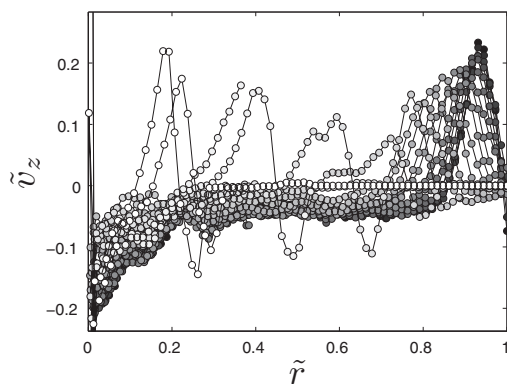
Fig. 5. Vertical component of the velocity $\tilde{v}_z$ as a function of the distance $\tilde{r}$ from the center, and at $z = 10\,\mu m$. Note that this component of the velocity is deduced from v_r with mass conservation: $\partial_z v_z = -\partial_r(rv_r)/r$ and assuming a constant shear rate closed to the surface, v_z is given by $v_z \simeq -z\partial_r(rv_r)/r$.
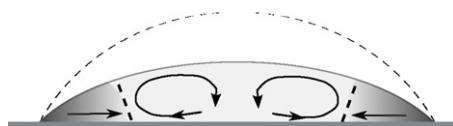
Fig. 6. Scheme of the flow inside the drying droplet: in the fluid central zone, there is a recirculating flow, and in the gelled corner an inward flow interpreting as a capillary creeping.

above 5% and seems to diverge around 8–9% [10], it is tempting to interpret the slowing down of the Marangoni flow as mainly due to the increase in the mean viscosity of the suspension. Please also note that the beginning of the intermediate regime coincides with the fact that the deposit is growing significantly, as shown in Fig. 3. The velocity profiles displayed in Fig. 4 also show that the decrease in the mean velocity is partly due the fact that the fluid recirculating zone is reduced due the growing of the deposit and to the fact that, in the deposit, the radial velocity is *negative*.

An other interesting feature is the fact that the sense of the recirculation remains does not change until the end of the drying (expect for the most concentrated solutions at late times, see Fig. 4). This is in apparent contradiction with some theoretical predictions which expect a change in the sign of the thermal Marangoni stress when the contact angle decreases below a finite value [4,12,6]. For water on thin glass plate, this value is however quite low ($\sim 10°$ [12]) an would only be reached during the last stage of the drying, where the droplet is very inhomogeneous. Let us recall that the prediction holds for pure liquids and account neither for the change in time of the effective properties of the sol nor for concentration gradients.

Let us finally come back to the observation that the velocity in the deposit is non-zero and *negative*, i.e., there is a movement of the tracers from the edge to the center. This is observed *for all the droplets* tested, and reaches rather high values at the end of

the drying (see Fig. 4). These very late times are rather difficult to interpret since at these times, we observe that the deposit progressively delaminates. The self-diffusion coefficient of the tracers in the deposit is below the detection limit, showing that the effective viscosity is very high (above 1 Pa s). It is thus rather surprising to observe negative and significant velocities. Although the viscosity is high, let us recall that the concentration remains low ($\sim$8–9%), so that the elastic modulus of the gelled phase should be rather low, probably on the order of 1–10 Pa. Such values are below or on the same order of the capillary pressure, which implies that surface tension should be able to deform the deposit. It is thus *creeping* under the capillary stress exerted by the interface, as sketched in Fig. 6. Whether the foot of the drop keeps exactly the spherical-cap shape as depicted in Fig. 6 or it partially prevents the drop to shrink and exhibits a well-known foot effect [13] is still unclear and could be evidenced using dedicated time-resolved three-dimensional confocal imaging at the level of the foot [14].

4. Conclusion

This work ask for a deeper theoretical work concerning Marangoni flows in drying droplets whose properties evolves with time. Indeed, we note that the rheology of the suspension plays a significant role that not only obviously impacts the hydrodynamics in the drop but also possibly overcomes the expected effects due to heat transfers calculated for pure liquids.

Beside, we observe of a *creeping in the deposit* which is fascinating and rarely described. Understanding the limiting regimes of this creeping is an important challenge because it affects the overall drying mechanism [15] and could also be an additional mean to control specific deposition patterns by tuning the elastic properties of the deposit.

References

[1] E. Tekin, B.J. de Gans, U.S. Schubert, Journal of Materials Chemistry 14 (2004) 2627–2632.
[2] B.G. Prevo, D.M. Kuncicky, O.D. Velev, Colloids and Surfaces A: Physicochemical and Engineering Aspects 311 (2007) 2–10.
[3] R.D. Deegan, O. Bakajin, T.F. Dupont, G. Huber, S.R. Nagel, T.A. Witten, Nature 389 (1997) 827–829.
[4] H. Hu, R.G. Larson, Langmuir 21 (2005) 3963–3971.
[5] H. Hu, R.G. Larson, Journal of Physical Chemistry B 110 (2006) 7090–7094.
[6] W.D. Ristenpart, P.G. Kim, C. Domingues, J. Wan, H.A. Stone, Physical Review Letters 99 (2007) 234502.
[7] Y. Hamamoto, J.R.E. Christy, K. Sefiane, Physical Review E 83 (2011) 051602.
[8] X.F. Xu, J.B. Luo, Applied Physics Letters 91 (2007).
[9] T. Kajiya, D. Kaneko, M. Doi, Langmuir 24 (2008) 12369–12374.
[10] H. Bodiguel, J. Leng, Soft Matter 6 (2010) 5451–5460.
[11] G. Berteloot, A. Hoang, A. Daerr, H.P. Kavehpour, F. Lequeux, L. Limat, Journal of Colloid and Interface Science 370 (2012) 155–161.
[12] X.F. Xu, J.B. Luo, D. Guo, Langmuir 26 (2010) 1918–1922.
[13] Y. Gorand, L. Pauchard, G. Calligari, J.P. Hulin, C. Allain, Langmuir 20 (2004) 5138–5140.
[14] H. Li, N. Fowler, C. Struck, S. Sivasankar, Soft Matter (2011).
[15] Y.O. Popov, Physical Review E 71 (2005) 036313.